Plant-Microbe Interfaces: Characterization of IAA biosynthesis pathways in *Populus*-associated microbes

Jennifer Morrell-Falvey[1,3,6*] (morrelljl1@ornl.gov), David Garcia[2], Kasey Estenson[3], Miriam Land[1], Xiaolin Cheng[4], Gregory Hurst[5], Robert Standaert[1,6], Amber Bible[6], and Mitchel Doktycz[1,2]

[1]Biosciences Division, Oak Ridge National Laboratory, [2]Bredesen Center, University of Tennessee, [3]UT-ORNL Graduate School of Genome Science and Technology, University of Tennessee, [4]Medicinal Chemistry and Pharmacognosy, The Ohio State University, Columbus, OH; [5]Chemical Sciences Division, Oak Ridge National Laboratory, [6]Department of Biochemistry & Cellular and Molecular Biology, University of Tennessee

Abstract

Populus deltoides **(poplar) hosts a diverse microbiome that influences its growth and productivity. Many plant-associated bacteria have the ability to produce phytohormones, such as indole-3-acetic acid (IAA). However, elucidating the pathways associated with secondary metabolite production in microorganisms is an ongoing challenge. Multiple IAA biosynthetic pathways have been described in microbes, most of which require the precursor tryptophan. The tryptophan-dependent pathways include the indole-3-acetonitrile (IAN) pathway, the indole-3-acetamide (IAM) pathway, the tryptophan side-chain oxidase (TSO) pathway, the indole-3-pyruvate (IPA) pathway, and the tryptamine pathway. We are pursuing the use of cell-free metabolic engineering coupled with bioinformatic searches of genome databases and protein-ligand docking simulations in order to predict the proteins most likely to be involved in a metabolic pathway. In particular, genomic analysis was used to predict that *Pantoea* sp. YR343 synthesizes IAA using the indole-3-pyruvate (IPA) pathway. This prediction was tested using a combination of proteomics, metabolomics and genetics. To better understand IAA biosynthesis and the effects of IAA exposure on cell physiology, we characterized proteomes of *Pantoea* sp. YR343 grown in the presence of tryptophan or IAA. These data indicate that indole-3-pyruvate decarboxylase (IpdC), a key enzyme in the IPA pathway, is upregulated in the presence of tryptophan and IAA. Metabolite profiles of wildtype cells showed the production of IPA, IAA, and tryptophol, which is also consistent with an active IPA pathway. Finally, we constructed a mutant in *Pantoea* sp. YR343 in which the *ipdC* gene was deleted. This mutant was unable to produce tryptophol, consistent with a loss of IpdC activity, but was still able to produce IAA (20% of wildtype levels). This result suggests the possibility of an alternate pathway or the production of IAA by a non-enzymatic route. To examine this possibility and to aid in the assignment of candidate enzymes in the pathways, we employed protein-ligand docking simulations. The resulting computationally predicted set of enzymes were then expressed and tested in cell free systems for their ability to produce IAA.**

Predicted IAA biosynthetic pathways in *Pantoea* sp. YR343 based on genomic analyses

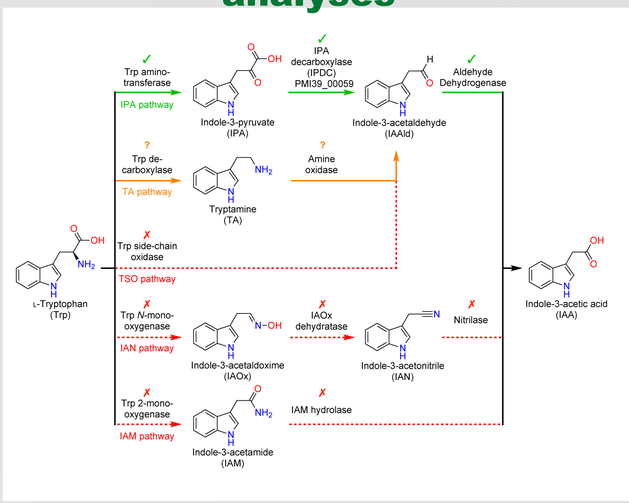

Figure 1. Tryptophan-dependent IAA biosynthetic pathways in *Pantoea* sp. YR343. The pathways are color-coded based on genomic analyses with green lines and checks indicating the presence of genes encoding candidate enzymes for each step in the pathway, orange lines and question marks indicating the presence of possible candidate gene products, and red lines with exes indicating the absence of genes encoding candidate enzymes for the pathway.

IAA biosynthetic pathway analyses using proteomics

Genomic analyses predicts that *Pantoea* sp. YR343 may have a functional IPA pathway. We identified a gene (PMI39_00059; *ipdC*) that encodes indole-3-pyruvate decarboxylase (IpdC), an enzyme in the IPA pathway that catalyzes the committed step. The first step in the IPA pathway (Trp→IPA) requires an aromatic aminotransferase and we identified seven genes in *Pantoea* sp. YR343 that are annotated to encode gene products with this function (Table 1). Likewise, the final step in this pathway (indole-3-acetaldehyde (IAAld) →IAA) requires an aldehyde dehydrogenase and we found 17 gene products annotated with this function (Table 1). Proteomic analyses was used to investigate which of these proteins are expressed during growth in the presence of the precursor tryptophan or IAA itself.

	Candidate Enzymes in IAA Biosynthesis				
	Indole-3-Pyruvate Pathway				
	LocusTag	log2ratio Trp: Glu	log2ratio IAA1ug:Glu	log2ratio IAA10ug:Glu	log2ratio IAA100ug:Glu
	Aromatic aminotransferases				
1	PMI39_01811	0.8	0.4	0.8	1.1
	PMI39_01993	0.2	0.07	0.4	-0.3
	PMI39_02094	-1.4	-2	-0.9	down
2	(PMI39_02628)	NA	(up)	(up)	(up)
	(PMI39_02920)	NA	NA	NA	NA
	(PMI39_04274)	NA	NA	NA	(up)
	PMI39_04560	0.6	0.7	0.2	1.1
	Indole-3-pyruvate decarboxylase (IpdC)				
3	PMI39_00059	up	NA	(up)	up
	Aldehyde Dehydrogenases				
	(PMI39_0031	NA	NA	NA	NA
	(PMI39_00317)	NA	NA	NA	NA
	PMI39_00354	-0.4	0.3	0.4	0.2
5	(PMI39_00431)	NA	NA	NA	NA
	PMI39_00617	-0.7	-2	0.3	1.1
6	(PMI39_00725)	NA	(up)	(up)	(up)
7	(PMI39_00794)	NA	(up)	NA	NA
8	(PMI39_00977)	NA	NA	NA	NA
9	(PMI39_01356)	NA	(up)	NA	NA
	PMI39_02144	-0.03	1.1	1.7	0.9
	PMI39_02889	0.6	0.3	0.4	1.4
10	PMI39_03367	-0.6	-0.4	-0.2	0.6
	(PMI39_03939)	NA	NA	NA	NA
11	PMI39_04111	0.4	0.09	0.6	0.4
12	(PMI39_04199)	(down)	(down)	1	(down)
13	(PMI39_04201)	(down)	(down)	(down)	(down)
	PMI39_04236	-0.02	0.03	-0.2	0.2
	Tryptamine Pathway				
	PMI39_03119	-0.3	1.9	2	2.5
	PMI39_00935	NA	NA	NA	NA
	PMI39_02858	NA	NA	NA	NA

Table 1. Candidate enzymes in the IAA biosynthetic pathways. Proteomics data in the body of the table are $\log_2$-transformed NSAF ratios of experimental condition shown in the column header to control (minimal media). Highlighted ratios indicate differential abundance between treatment and control. Values of "up" or "down" are shown where a protein was not detected in either the treatment or control, so that an accurate ratio could not be calculated. Parentheses around "up" or "down" indicate that a protein fell below the low-abundance threshold for both treatment and control. Parentheses around a Locus Tag indicate that the protein fell below the low abundance threshold for all proteome measurements.

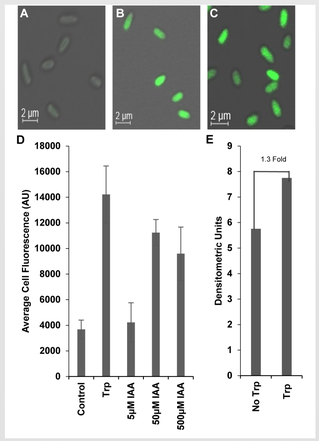

Figure 2. Induction of *ipdC* gene expression in *Pantoea* sp. YR343. Images of cells harboring the pPROBE-*ipdC* reporter plasmid (A) before or (B) after growth in the presence of tryptophan or after growth in the (C) presence of 50 μM IAA. (D) Graph of average cell fluorescence from wildtype *Pantoea* sp. YR343 cells harboring pPROBE-ipdC grown under different conditions: no Trp (control),1 mM Trp, 5 μM IAA, 50 μM IAA, or 500 μM IAA. The fluorescence of 60 cells was averaged for each treatment. E) Comparison of *ipdC* gene expression using RT-PCR after growth in the absence or presence of tryptophan. *ipdC* gene expression was normalized against 16S RNA as a control.

Metabolite profiles of wildtype and Δ*ipdC* mutant

We next constructed a mutant strain of *Pantoea* sp. YR343 in which the *ipdC* gene was disrupted and we analyzed culture media from both wild-type and Δ*ipdC* mutant cells for IAA and other metabolites using GC/MS. The dominant Trp metabolites in wildtype supernatants were IPA, tryptophol (TOL), and indole-3-lactate (ILA), with smaller amounts of IAA and indole-3-carboxyaldehyde. In the absence of *ipdC*, the dominant metabolites were indole-3-pyruvate and indole-3-lactate (Figure 3). Tryptophol was completely absent in the supernatant from these mutant cells. Since tryptophol is produced from IAAld, we conclude that the Δ*ipdC* mutant lacks indole-3-pyruvate decarboxylase activity and is unable to produce IAAld. Interestingly, however, we did detect some IAA in the mutant cells, albeit at much lower levels compared to wild type cells (500 ng/ml; 20% of wildtype levels). As in the wildtype cells, we failed to detect IAN, IAM, or TA (Figure 3).

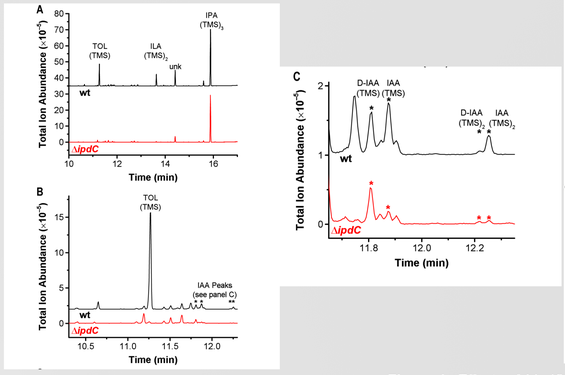

Figure 3. Indole metabolite analysis of *Pantoea* sp. YR343 and *Pantoea* sp. YR343 Δ*ipdC* by GC/MS. A) Total ion current chromatogram B) scale expansion of TOL region C) scale expansion of IAA region. IAA produced variable mixtures of single and double trimethylsilyl (TMS derivatives), resulting in two peaks. IAA-d_7 (D-IAA) at 1 μg/mL was added as an internal standard for IAA.

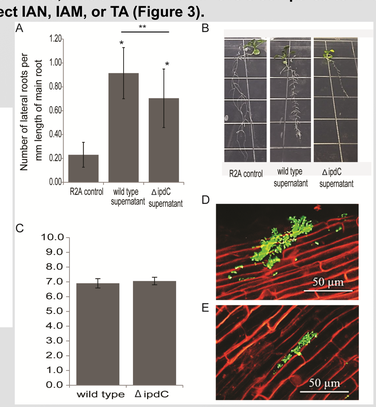

Figure 4. Effects of Δ*ipdC* mutant on plants. (A) Lateral root density was measured as the number of lateral roots per mm of main root length. Images were analyzed using ImageJ and statistics were calculated using the Student's t-test ($p < 0.05$). *, significant difference when compared to the control. **, significant difference between treatment with wild type supernatant and Δ*ipdC* supernatant. (B) Representative images of *A. thaliana* seedlings after one week treatment with culture supernatants from wild type *Pantoea* sp. YR343 and the Δ*ipdC* mutant. (C) Colonization experiments with *P. trichocarpa*. Wild type *Pantoea* sp. YR343 and the Δ*ipdC* mutant were measured as the $\log_{10}$ value of colony forming units (CFU) per gram of root material. No significant differences were observed. (D, E) Representative images of *P. trichocarpa* root colonization by (D) wildtype YR343:GFP or (E) mutant Δ*ipdC*:GFP. Bacteria were detected by GFP fluorescence (green) and *P. trichocarpa* roots were detected by autofluorescence (red).

Pathway analyses via computation and cell-free metabolic engineering

This method is broadly described in three steps (Figure 5). First, we perform bioinformatic analyses of the genomes of interest using query enzymes to find homologous enzymes and potentially complete pathways. Second, we perform ligand-docking simulations using AutoDock Vina to further cull the list enzymes to those most effectively able to interact with their predicted ligands. Third, we utilize a cell-free metabolic engineering system with extracts enriched for individual nodes in the predicted IAA pathways. The results were used to effectively reduce the list candidate enzymes most likely to be active in *Pantoea* sp. YR343.

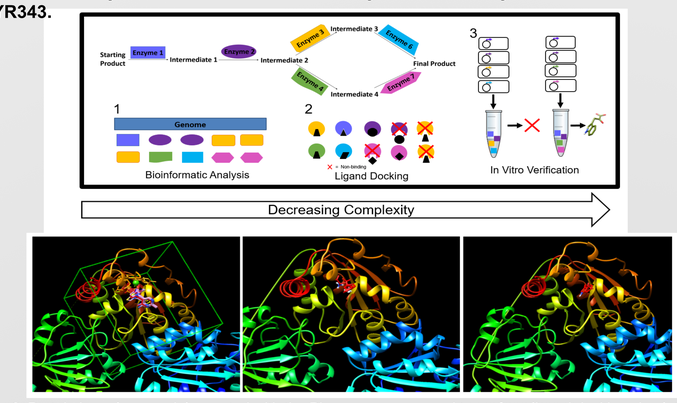

Figure 6. Protein homology models created with the Phyre server are used to perform ligand docking simulations using AutoDock Vina. Ligand binding site predictions helped inform docking parameters. Images above are representative of the experiment, but specific to PMI39_00059 IPDC. A. Ligand site predictions are used to designate the search space used by AutoDock Vina. B. Each protein was docked with a decoy (L-phenylalanine) C. and its expected binding partner, in this case indole pyruvate for PMI39_00059.

	Am-TRF	IPDC	IAALDh	Total
Bioinformatic Analysis	2	2	17	68
Ligand Docking	2	1	9	18

Table 2. Each step in the INCAPD process eliminates enzymes based on the prescribed parameters. Below each enzyme are the total number of peptides to be used for the downstream step.

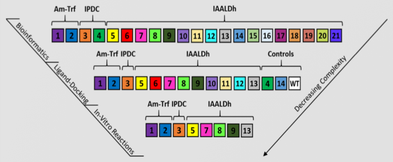

Figure 7. Each step in the process generates fewer potential pathways to produce IAA. The decreasing complexity of the search space thereby limits the amount of time that must be spent exploring each pathway empirically. Each number corresponds to a single enzyme for the first step in the pathway aminotransferase (Am-Trf), the second step Indole-3-pyruvate dehydrogenase, and the third step Indole-acetaldehyde dehydrogenase (IAALDh). The bioinformatic step designates enzymes from YR343 left after BLAST, the Ligand-Docking step contains enzymes left after the use of Vina, and the In-vitro reactions step correspond to enzymes shown to be active in the production of IAA.

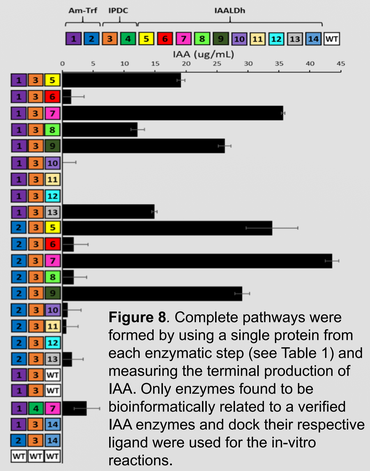

Figure 8. Complete pathways were formed by using a single protein from each enzymatic step (see Table 1) and measuring the terminal production of IAA. Only enzymes found to be bioinformatically related to a verified IAA enzymes and dock their respective ligand were used for the in-vitro reactions.

Conclusions and future directions

- **A combination of genomic, metabolomic, and proteomic analyses indicates that the indole pyruvate pathway is the major IAA biosynthetic pathway in *Pantoea* sp. YR343**
- **Disruption of the *ipdC* gene results in a significant decrease of IAA production. Whether this IAA is produced by non-enzymatic degradation of IPA or by an alternate route is unknown.**
- **We have coupled computational analyses and cell-free metabolic engineering to efficiently analyze biosynthetic pathways, which provides the ability to test a large set of potential pathways and cull those unlikely to produce the compound of interest.**
- **This computational and CFME method can be broadened to identify novel pathways or develop strategies to synthesize desired compounds.**
- ***Arabidopsis* seedlings treated with supernatant collected from WT and mutant cells produced different growth phenotypes. It will be interesting to test individual indolic compounds produced by *Pantoea* sp. YR343 to determine the effects on root growth and architecture.**
- **We found that Δ*ipdC* mutant cells were able to associate with poplar roots as efficiently as wildtype cells, suggesting that IAA production via the IPA pathway is not likely required for attachment to the root.**
- **To better understand plant-microbe association, we will need to measure the local concentration and spatial distribution of metabolites produced by microbes during plant association.**

Acknowledgement:

This research was funded by the US DOE Office of Biological and Environmental Research, Genomic Science Program. Oak Ridge National Laboratory is managed by UT-Battelle, LLC, for the US Department of Energy under Contract no. DEAC05-00OR22725.